Journal of Ecological Engineering

Journal of Ecological Engineering 2022, 23(1), 118–128
https://doi.org/10.12911/22998993/143908
ISSN 2299–8993, License CC-BY 4.0

Received: 2021.10.25
Accepted: 2021.11.15
Published: 2021.12.01

High Efficient Photocatalytic Degradation of Methyl Orange Dye in an Aqueous Solution by $CoFe_2O_4$-SiO_2-TiO_2 Magnetic Catalyst

Poedji Loekitowati Hariani[1*], Muhammad Said[1], Salni[2], Nabila Aprianti[3], Yohanna Asina Lasma Rohana Naibaho[1]

[1] Department of Chemistry, Faculty of Mathematics and Natural Sciences, Sriwijaya University, Jalan Palembang-Prabumulih, Indralaya, Ogan Ilir, Indonesia
[2] Department of Biology, Faculty of Mathematics and Natural Sciences, Sriwijaya University, Jalan Palembang-Prabumulih, Indralaya, Ogan Ilir, Indonesia
[3] Doctoral Program of Environmental Science, Graduate School, Sriwijaya University, Jalan Padang Selasa 524 Bukit Besar, Palembang 30139, South Sumatra, Indonesia
* Corresponding author's email: puji_lukitowati@mipa.unsri.ac.id

ABSTRACT

This study successfully synthesized a core-shell-shell in the form of $CoFe_2O_4$-SiO_2-TiO_2 catalyst magnetic and recyclable. The catalyst was employed for the photocatalytic degradation of methyl orange (MO) dye. Subsequently, the catalyst was subjected to XRD, FTIR, SEM-EDS, VSM, as well as UV-DRS characterizations. The photocatalytic degradation was studied as a function of the solution pH, MO concentration, and irradiation time, while the kinetics of photocatalytic degradation and the catalyst reusability were also evaluated. On the basis of the XRD, FTIR, and SEM-EDS characterizations, the $CoFe_2O_4$ coating was successfully carried out using SiO_2 and TiO_2. $CoFe_2O_4$-SiO_2-TiO_2 was discovered to possess magnetic properties with a saturation magnetization of 17.59 emu/g and a bandgap value of 2.4 eV. The photocatalytic degradation of MO followed the Langmuir-Hishelwood model. The optimum degradation was obtained at the MO concentration of 25 mg/L, solution pH of 4, catalyst dose of 0.05 g/L, irradiation time of 160 minutes, MO removal efficiency achieved 93.46%. The regeneration study showed $CoFe_2O_4$-SiO_2-TiO_2 after 5 cycles were able to catalyze the photocatalytic degradation with an MO removal efficiency of 89.96%.

Keywords: $CoFe_2O_4$-SiO_2-TiO_2, magnetic, degradation, photocatalytic, and methyl orange.

INTRODUCTION

The continuous discharge of industrial liquid waste containing toxic compounds into water bodies tends to cause environmental pollution and presents several health risks [Ojemaye et al., 2015]. The previous studies by Chan et al. [2008] and Trabelsi et al. [2016] described dyes as toxic compounds produced by several industries, including the textile, pharmaceutical, chemical, paper, foodstuff, soap, cosmetic, and leather industries, where over 50% of the dyes used are azo-based. According to Koohestani et al. [2016], azo dyes are the compounds with an azo bond in the form of -N=N-. Over 15% of the dyes are discharged as liquid waste during the dyeing and coloring process [Nair et al., 2014; Ahmad et al., 2014]. Azo dyes and their intermediates, for instance aromatic amines, are highly stable, toxic, carcinogenic, mutagenic, and not easily degraded [Konstantinou and Albanis, 2004; Alghamdi et al., 2019]. A report by Huang et al. [2008] showed that dyes block the penetration of light into the water, consequently lowering the photosynthetic efficiency and impeding the growth of aquatic organisms. These dyes also cause aesthetic changes which are harmful to the environment. Methyl orange (MO) is an azo dye with the molecular formula $C_{14}H_{14}N_3SO_3Na$ and is classified as an anionic dye with a sulfonic group. In addition to being used as an industrial coloring agent, MO is also used as a pH indicator in the laboratory, with a pH indicator range of 3.1 to 4.4 [Alghamdi et al., 2019].

Recently, advanced oxidative processes (AOPs) were discovered to be the most effective method for degrading organic matter from water and wastewater [Suzuki et al., 2015; Mrotek et al., 2020]. These processes are based on the formation of highly reactive radicals, including hydroxyl groups, which oxidize and convert organic compounds into harmless products, for instance, CO_2 and H_2O [Ge et al. 2019; Takdastan et al., 2018]. Heterogeneous photocatalysis using semi-conductors is an effective technique for the degradation of toxic organic compounds. In wastewater treatment, TiO_2 in various forms is a widely used photocatalyst due to the its ease and low cost of production, high photoactivity, non-toxicity, as well as good electrical and thermal conductivity [Shojaie et al., 2018; Stefan et al., 2016, Subramonian et al., 2017].

However, TiO_2 is suspended in a solution, which makes it difficult to separate and energy-consuming processes [Lee et al., 2001; Jorfi et al., 2017], electron-hole recombination of the photo-generated charge carriers [Pastravanu et al., 2014], as well as a wide bandgap (about 3.2 eV) [Djellabi et al., 2019]. Therefore, TiO_2 is only suitable for use under UV light to generate electron-hole pairs. Alternatively, magnetic photocatalysts in which semiconductor nanoparticles are deposited on the ferrite surface (Fe_3O_4, Fe_2O_4, $CoFe_2O_4$, $ZnFe_2O_4$), has been used to facilitate the separation of the photocatalyst from the solution, using an external magnet [Jurek et al., 2017, Mishra et al., 2019]. The coating of Fe_3O_4 as the core, with TiO_2, reduces the bandgap of TiO_2, making the compound suitable for the photocatalytic visible region while increasing the speed and efficiency of the separation process [Mercyrani et al., 2017]. However, direct contact between ferrite compounds and TiO_2 causes TiO_2 to enter the core oxidizing iron, and consequently, the ferrous ions dissolve into solution (photo-dissolution) [Gebrezgiabher et al., 2019; Wysocka et al., 2018]. According to Rashid et al. [2015] and Jurek et al. [2017], the formation of a layer on the magnetic core helps to prevent degradation, photo-dissolution, and adverse effects of the magnetic core on TiO_2. Silica protects the magnetic core, prevents the transmission of electron holes from the photocatalyst layer to the magnetic part, and is, therefore, often used as an intermediary [Awazu et al., 2008; Cheng et al., 2012].

In this study, a core-shell-shell in the form of $CoFe_2O_4/SiO_2/TiO_2$ was prepared as a photocatalyst for the degradation of MO. $CoFe_2O_4$ was selected as the core due to its high thermal and chemical stability, low toxicity, high coercivity, as well as moderate magnetization [Rajput and Kaur, 2014; El-Shobaky et al., 2010]. Subsequently, the photocatalytic efficiency of the degradation, including the effect of solution pH, irradiation time, as well as catalyst dose, were investigated, and the reusability of catalysts was evaluated.

MATERIAL AND METHODS

Materials

The study involved the use of cobalt chloride hexahydrate ($CoCl_2.6H_2O$), Iron(III) chloride hexahydrate ($FeCl_3.6H_2O$), Trisodium citrate dihydrate ($C_6H_5Na_3O_7.2H_2O$), ethanol (C_2O_5OH), Sodium hydroxide (NaOH), Hidrochlorid acid (HCl), Tetraethyl orthosilicate ($Si(OC_2H_5)_4$, Ammonium hidroxide (NH_4OH), Methyl orange ($C_{14}H_{14}N_3SO_3Na$), Titanium (IV) butoxide ($Ti(OCH_2CH_2CH_2CH_3)_4$, Ethylene glycol $(CH_2OH)_2$, Sodium nitrate ($NaNO_3$), Titanium dioxide (TiO_2) from Merck, Germany.

$CoFe_2O_4$ preparation

$CoFe_2O_4$ was synthesized using the coprecipitation method. For this process, 9.517 g of $CoCl_2.6H_2O$ and 21.623 g of $FeCl_3.6H_2O$ were dissolved in 100 mL of distilled water. Subsequently, 2 M NaOH was added to the solution in drops, while nitrogen gas was passed across until a pH of 10 was obtained. The precipitate obtained was then collected by magnetic separation, washed several times with distilled water until the pH was neutral, and oven-dried at 110 °C for 1 hour. This was followed by subjecting the $CoFe_2O_4$ obtained to further calcination at 800 °C for 2 hours.

$CoFe_2O_4$-SiO_2 preparation

The synthesis of $CoFe_2O_4$-SiO_2 was carried out using the sol-gel method. For this process, 0.8 g of $CoFe_2O_4$ and 0.8 g of Trisodium citrate dihydrate were dissolved in 20 mL of ethanol and

8 mL of distilled water. The mixture was then homogenized by sonification for 10 minutes, and 4 mL of ammonium hydroxide, as well as 3.2 mL of TEOS, were added to the solution, and sonification was continued for 3 hours at 40 °C to form a silica layer around $CoFe_2O_4$. Subsequently, the precipitate obtained was separated by centrifugation, washed severally with ethanol, and dried using rotary evaporation.

$CoFe_2O_4$-SiO_2-TiO_2 preparation

The $CoFe_2O_4$-SiO_2-TiO_2 composites were prepared using the method reported by Habila et al. [2015], with some modifications. For this process, 2 g of $CoFe_2O_4$-SiO_2 was suspended in a mixture of 24 mL ethanol, 30 mL distilled water, and 800 L ammonium hydroxide (28%), using sonification, for 30 minutes. Subsequently, 20 mL of ethylene glycol and 2 mL of TBT solution were slowly added and the mixture was homogenized using a magnetic stirrer at 45 °C, for 24 hours. The $CoFe_2O_4$-SiO_2-TiO_2 obtained was washed with distilled water, as well as ethanol, then oven-dried at 110 °C for 1 hour and calcined at 450 °C for 3 hours.

Characterization

The crystal structure and phase of catalyst were analyzed using X-Ray Diffraction (XRD PANalytical), while the functional groups were identified using Fourier Transform Infra-Red (FTIR Prestige 21 Shimadzu). In addition, the morphology and elemental composition were analyzed using a Scanning Electron Microscope-Energy Dispersive Spectrometer (SEM-EDS JOEL JSM 6510 LA). The magnetic moment was determined using a Vibrating Sample Magnetometer (VSM Oxford Type 1.2 T). At the same time, the wavelength and band gap were analyzed using Diffuse Reflectance Ultra Violet-Visible Spectroscopy (UV-Vis DRS Pharmaspec UV-1700). The radiation source for photocatalytic degradation was UV light (12 W Phillips) and the MO absorbance was measured using a UV-Vis Spectrophotometer (Type Orion Aquamate 8000). Mineralization degree was measurement by Total Organic Carbon (TOC Teledyne Tekmar). Determination of pHpzc was carried out following a modification of the technique reported by Bezahdi et al. [2020] using $NaNO_3$ solution as an electrolyte.

Photocatalytic degradation

In this experiment, 50 mL of MO was mixed with $CoFe_2O_4$-SiO_2-TiO_2 at a dose of 0.05 g/L in separate quartz pipes, with the MO concentrations of 25, 50, 75, and 100 mg/L. Using UV light as the irradiation source, the mixture was placed in a photoreactor with a vessel distance of 30 cm from the light source. Furthermore, the effects of the pH and irradiation time were studied by varying the pH in the range of 2 to 7, as well as the irradiation time between 0 to 200 minutes. Subsequently, the MO removal (%) was calculated using the following formula (Eq. 1).

$$\text{MO Removal (\%)} = \frac{C_o - C_t}{C_o} \quad (1)$$

where: C_o and C_t are the initial and final concentrations of MO (mg/L).

The reusability of the catalyst was also investigated using the same method, under the optimum conditions for photocatalytic degradation. For this evaluation, the $CoFe_2O_4$-SiO_2-TiO_2 was separated using a permanent magnet after the photocatalytic degradation, then washed with ethanol and distilled water, dried in an oven for 60 minutes at 80 °C, and reused for photocatalytic degradation [Ajabshir and Niasari, 2019]. This experiment was repeated 5 times, and the catalyst efficiency was measured after each cycle.

RESULT AND DISCUSSION

Properties of the materials

Figure 1 shows the XRD spectra of the synthesized $CoFe_2O_4$, $CoFe_2O_4$-SiO_2, and $CoFe_2O_4$-SiO_2-TiO_2. On the basis of the diagram, the 2θ angle of $CoFe_2O_4$ was observed at 30.31º (220), 35.57º (311), 43.21º (400), 53.61º (422), 57.23º (511), and 62.81º (440). This peak is a characteristic of the cubic spinel structure phase following the standard $CoFe_2O_4$ spectra (JCPDS card No. 78–1744). Meanwhile, $CoFe_2O_4$-SiO_2 was discovered to possess the same diffraction angle as $CoFe_2O_4$, but with lower peak intensity. Furthermore, the crystalline properties of $CoFe_2O_4$ were maintained after coating with SiO_2. The peak for SiO_2 at 2θ =15–25 was not observed in the XRD spectra of $CoFe_2O_4$-SiO_2 and $CoFe_2O_4$-SiO_2-TiO_2,

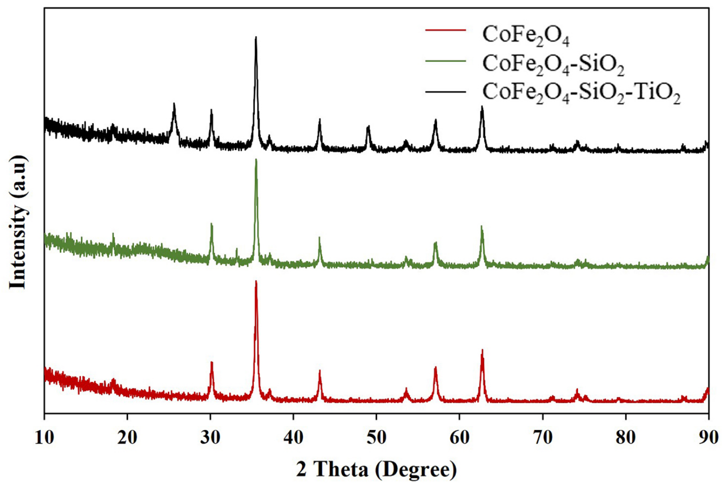

Figure 1. XRD spectra of (a)$CoFe_2O_4$ (b) $CoFe_2O_4$-SiO_2 and (c) $CoFe_2O_4$-SiO_2-TiO_2

due to the amorphous nature of SiO_2. Habila et al. [2020] reported a similar pattern in the synthesis of Fe_3O_4/SiO_2/TiO_2, where a reduction occurred in the Fe_3O_4 diffraction peak after coating with SiO_2 and TiO_2, due to the shielding effect of the two compounds.

The XRD spectra of $CoFe_2O_4$-SiO_2-TiO_2 shows the presence of a 2θ angle, which is characteristic of TiO2 at 25.63 (101), 37.25 (004), 48.87 (200), and 62.91 (204), based on the anatase phase structure (JCPDS card No. 21–1272). Table 1 shows the average crystallite size of $CoFe_2O_4$, $CoFe_2O_4$-SiO_2, and $CoFe_2O_4$-SiO_2-TiO_2 calculated by the Scherrer formula. The crystallite size of $CoFe_2O_4$ before and after coating remained at a constant value of ± 33 nm. Meanwhile, the average crystal size of TiO_2 calculated at the peak of the anatase diffraction was 18.3 nm.

Figure 2 shows the FTIR spectra of $CoFe_2O_4$, $CoFe_2O_4$-SiO_2, and $CoFe_2O_4$-SiO_2-TiO_2. The wavenumbers observed at about 3400 cm^{-1} and 1630 cm^{-1} in all spectra are stretching vibrations of the hydroxyl functional group (O-H) originating from free water molecules on the catalyst surface [Ojemaye et al., 2017]. Meanwhile, the $CoFe_2O_4$ spectra in the form of sharp peaks at 576 cm^{-1} are the vibrations of Fe-O. The strong peak at 1093 cm^{-1} observed in $CoFe_2O_4$-SiO_2, and $CoFe_2O_4$-SiO_2-TiO_2, is an asymmetric vibration of Si-O-Si [Fu et al., 2019], while the wavenumber around 950 cm^{-1} is the vibration of the Si-O-H band [Mortazavi et al., 2017]. According to Fu et al., [2019], the presence of TiO_2 in the $CoFe_2O_4$-SiO_2-TiO_2 spectra visible at 450 to 700 cm^{-1}, is the vibration of Ti-O-Ti and Ti-O-Si.

Table 1. The average crystallite size of $CoFe_2O_4$, $CoFe_2O_4$-SiO_2 dan $CoFe_2O_4$-SiO_2-TiO_2

Materials	Average crystallite size (nm)	
	$CoFe_2O_4$	TiO_2
$CoFe_2O_4$	33.24	-
$CoFe_2O_4$-SiO_2	33.40	-
$CoFe_2O_4$-SiO_2-TiO_2	33.34	18.24

The SEM and EDS analyses are used to investigate the morphology and composition of the catalyst elements. Figure 3 shows the morphology of $CoFe_2O_4$, $CoFe_2O_4$-SiO_2, and $CoFe_2O_4$-SiO_2-TiO_2 with the same magnification. The morphology of $CoFe_2O_4$ appears spherical because due to the small size which tends to agglomerate and the morphology of $CoFe_2O_4$-SiO_2 is similar to $CoFe_2O_4$ but more homogeneous. This is consistent with the XRD results which show the SiO_2 coating is not observed in the spectra due to the amorphous nature of the compound. Meanwhile, a heterogeneous and rough surface is visible in the morphology of $CoFe_2O_4$-SiO_2-TiO_2 where the TiO_2 aggregates appear to be round and coat the $CoFe_2O_4$-SiO_2. Table 2 shows the elemental composition of $CoFe_2O_4$, $CoFe_2O_4$-SiO_2, and $CoFe_2O_4$-SiO_2-TiO_2 from the EDS analysis, where the presence of Si and Ti elements in $CoFe_2O_4$-SiO_2-TiO_2 indicates a successful synthesis. Furthermore, no other elements were detected as impurities.

Figure 4 shows the magnetization curves of $CoFe_2O_4$, $CoFe_2O_4$-SiO_2, and $CoFe_2O_4$-SiO_2-TiO_2 obtained using VSM. According to the results, the saturation magnetization of $CoFe_2O_4$ is 57.05 emu/g, and this value is close to the saturation magnetization of $CoFe_2O_4$ synthesized using the combustion, coprecipitation, and precipitation methods, which are 56.7, 55.8, and

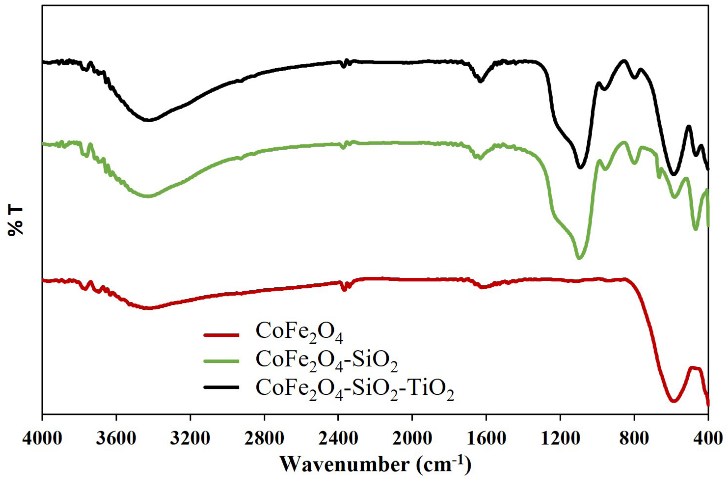

Figure 2. FTIR spectra (a)$CoFe_2O_4$ (b) $CoFe_2O_4$-SiO_2 and (c) $CoFe_2O_4$-SiO_2-TiO_2

47.2 emu/g, respectively [Houshiar et al., 2014]. In addition, the saturation magnetization of $CoFe_2O_4$-SiO_2 and $CoFe_2O_4$-SiO_2-TiO_2 are 40.01 emu/g, as well as 17.59 emu/g, respectively, and these values are lower, compared to the $CoFe_2O_4$ counterpart. This means that coating with non-magnetic material leads to a reduction in saturation magnetization. However, $CoFe_2O_4$-SiO_2-TiO_2 still has possessed good magnetic properties, considering the material is quickly and easily separated from the solution after degradation, using a permanent magnet.

a)

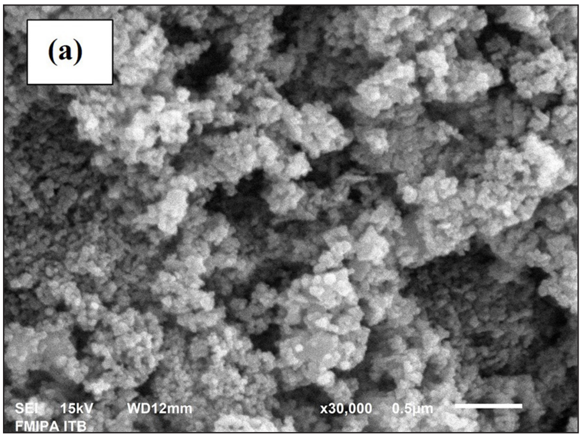

b)

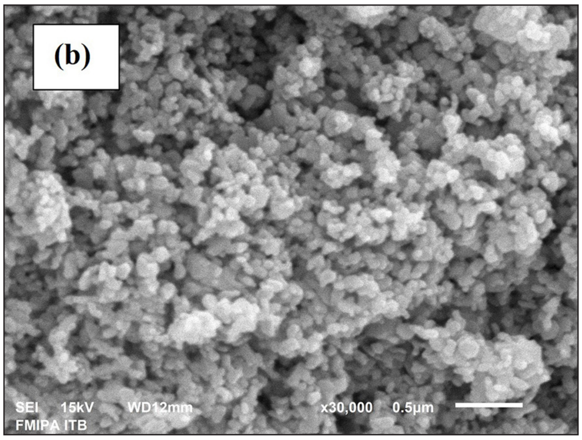

c)

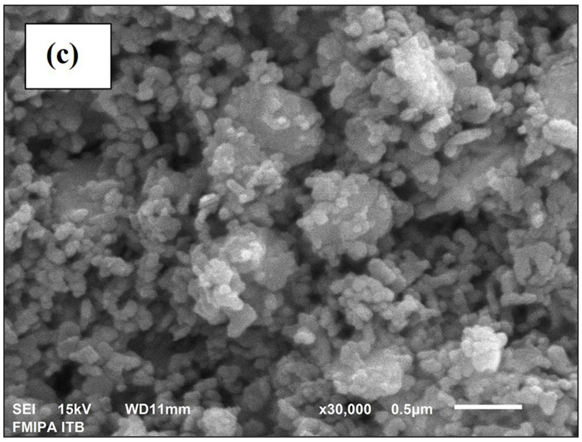

Figure 3. Morphology of (a) $CoFe_2O_4$ (b) $CoFe_2O_4$-SiO_2 and (c) $CoFe_2O_4$-SiO_2-TiO_2

Table 2. Elements of $CoFe_2O_4$, $CoFe_2O_4$-SiO_2 dan $CoFe_2O_4$-SiO_2-TiO_2

Elements (%)	Materials		
	$CoFe_2O_4$	$CoFe_2O_4$-SiO_2	$CoFe_2O_4$-SiO_2-TiO_2
O	19.43	23.27	26.18
Co	27.76	28.77	23.19
Fe	52.81	44.63	37.63
Si	-	3.32	12.25
Ti	-	-	0.75

Furthermore, Figures 5a and b show the UV-DRS spectra of $CoFe_2O_4$-SiO_2-TiO_2 and pure (commercial) TiO_2, which provide the information about the wavelength at which the catalyst absorbs energy. The results showed TiO_2 absorbs in the ultraviolet region with a maximum absorbance of about 345 nm, and this activity is due to the fairly large bandgap. Meanwhile, $CoFe_2O_4$-SiO_2-TiO_2 not only absorbs in the ultra-visible region but also in the visible region, at wavelengths of 341 and 425 nm, respectively. The bandgap value was obtained by plotting $(\alpha h\nu)^2$ against hν (Figure 5b). A TiO_2 band gap of 3.2 eV was obtained, and coating $CoFe_2O_4$ with SiO_2 and TiO_2 reduces the bandgap. Therefore, $CoFe_2O_4$-SiO_2-TiO_2 has a bandgap of 2.4 eV. According to Sonu et al., (2019), $CoFe_2O_4$ has a fairly small bandgap (~1.76 eV).

Photocatalytic properties

In photocatalytic degradation, the solution pH influences the charge of the catalyst surface. The solution pH is an important parameter. A report by Behzadi et al. [2020] showed the optimum pH depends on the type of pollutant and the pHpzc, which shows the pH on the material surface in total is zero or the catalyst surface is neutrally charged [Amulya et al., 2020]. The pHpzc value must be investigated to determine the appropriate pH for an effective photocatalytic degradation process. The pHpzc of $CoFe_2O_4$-SiO_2-TiO_2 is 5.2.

Figure 7 shows the effect of solution pH on the removal of MO, which has a pH range of 3.1–4.4 with a pKa of 3.7. At a solution pH < pHpzc, $CoFe_2O_4$-SiO_2-TiO_2 is positively charged, while MO is an anionic dye, and consequently, the attraction is more effective. MO removal increases at pH 2 to 4 and subsequently decreases at pH 5. Meanwhile, at a solution pH > pHpzc, there is a repulsion of electrostatic charges between the anionic dye and the negatively charged $CoFe_2O_4$-SiO_2-TiO_2. The highest MO removal was obtained at pH 4 with variations in the initial MO concentrations of 25, 50, 75, and 100 mg/L.

Figure 8 shows the effect of irradiation time on the photocatalytic degradation of MO at concentrations of 25, 50, 75, and 100 mg/L, the catalyst dose of 0.05 g/L, as well as pH of 4, under UV light. The results showed MO removal increases along with irradiation time; however, at 160 minutes of irradiation, there was no increase in the amount of degraded MO. Furthermore, the highest MO removal was obtained at a concentration of 25 mg/L (93.46%). This is because higher concentrations tend to block light from reaching the catalyst, consequently, reducing the rate of removal.

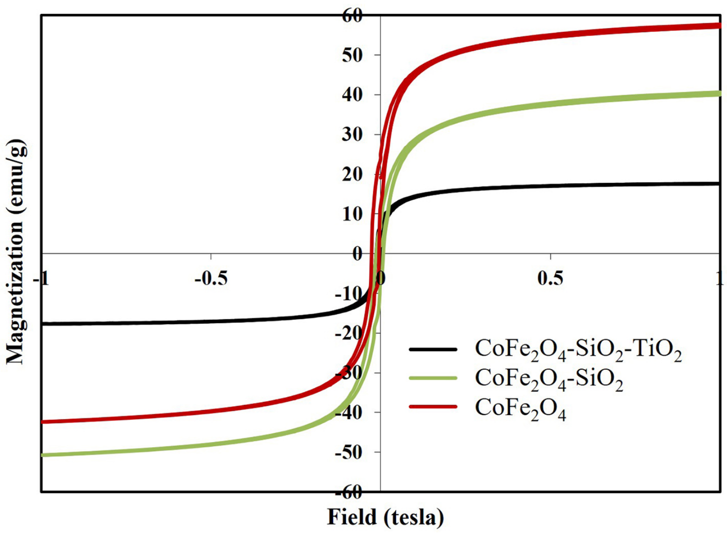

Figure 4. Saturation magnetization curves of (a) $CoFe_2O_4$, (b) $CoFe_2O_4$-SiO_2 and (c) $CoFe_2O_4$-SiO_2-TiO_2

a) b)

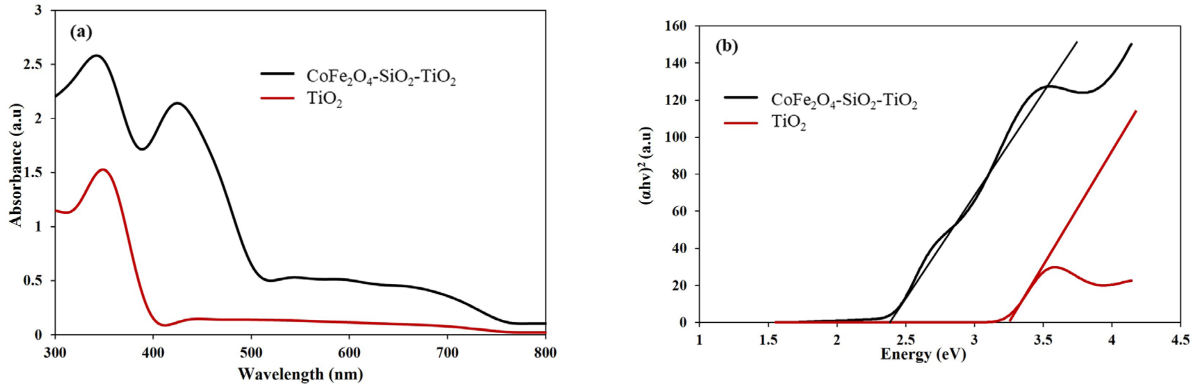

Figure 5. (a) UV-DRS spectra of $CoFe_2O_4$-SiO_2-TiO_2 and pure TiO_2 and (b) band gab of $CoFe_2O_4$-SiO_2-TiO_2 and pure TiO_2

The Langmuir Hinshelwood equation model is generally used to describe the kinetics of heterogeneous photocatalytic degradation. This equation is further simplified to pseudo-first-order kinetics to obtain the following equation (Eq. 2) [Amulya et al., 2020]:

$$\ln\left(\frac{C}{C_0}\right) = -kt \quad (2)$$

where: C_o and C are the initial concentration and the concentration after the photocatalytic degradation process, respectively, at a time (t).

Figure 8 shows the photocatalytic degradation kinetics of MO at concentrations of 25, 50, 75, and 100 mg/L, catalyst dose of 0.05 g/L, as well as pH of 4, under UV light. The concentrations produced R^2 values indicating the photocatalytic degradation has adequate linearity and follows the Langmuir-Hinshelwood model expressed in pseudo-first-order. Similar results were reported for the photocatalytic degradation of the Methylene blue dye using TiO_2-Fe_3O_4-bentonite [Chen et al., 2015], as well as the photocatalytic degradation of Cr(VI) using $NiFe_2O_4$-SiO_2-TiO_2 [Ojemaye et al., 2017]. Table 3 shows the kinetics parameters of MO photocatalytic degradation where the $t_{1/2}$ value is calculated using 0.693/k.

Reusability of the photocatalyst

The regenerability and reusability of catalysts are highly significant in industrial contexts, because these properties are related to cost, pilot-scale remediation systems, and environmental safety [Moosavi et al., 2020T; Ajabshir and Niasari, 2020]. Reusing catalysts reduces the

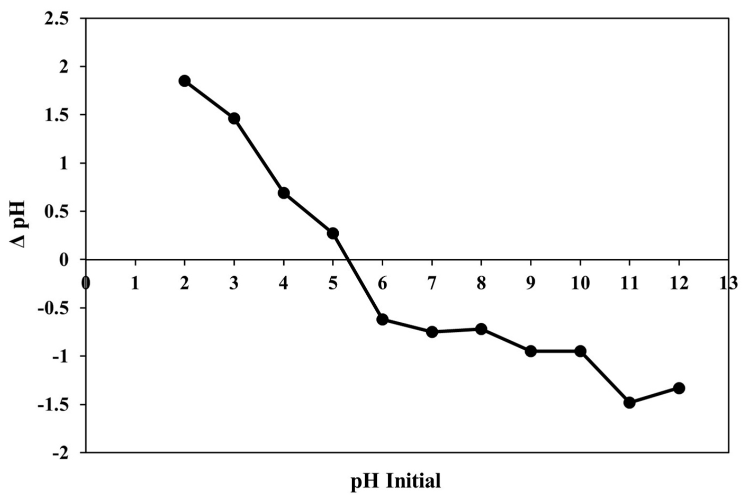

Figure 6. pHpzc of $CoFe_2O_4$-SiO_2-TiO_2

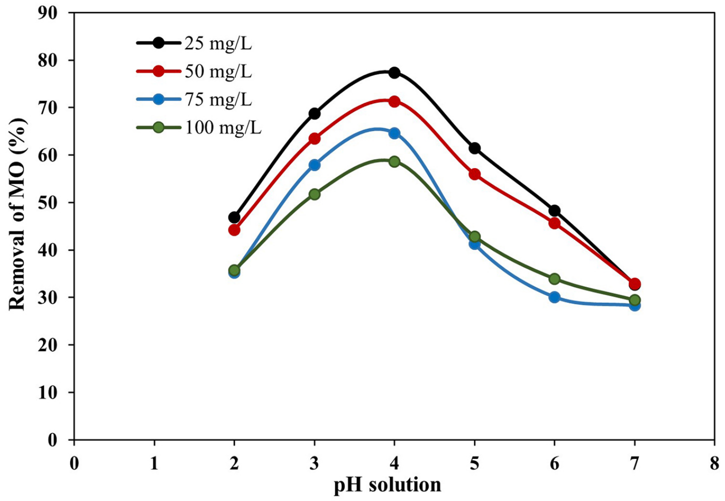

Figure 7. Effect of solution pH on removal MO

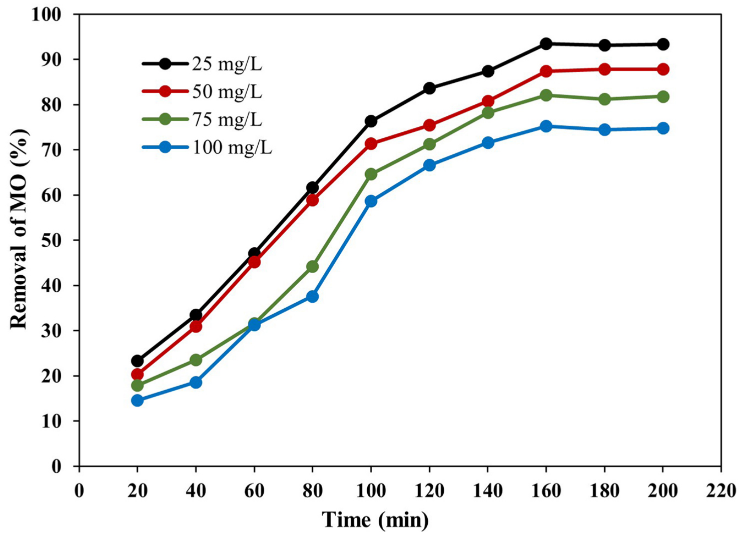

Figure 8. Effect of irradiation time on removal MO

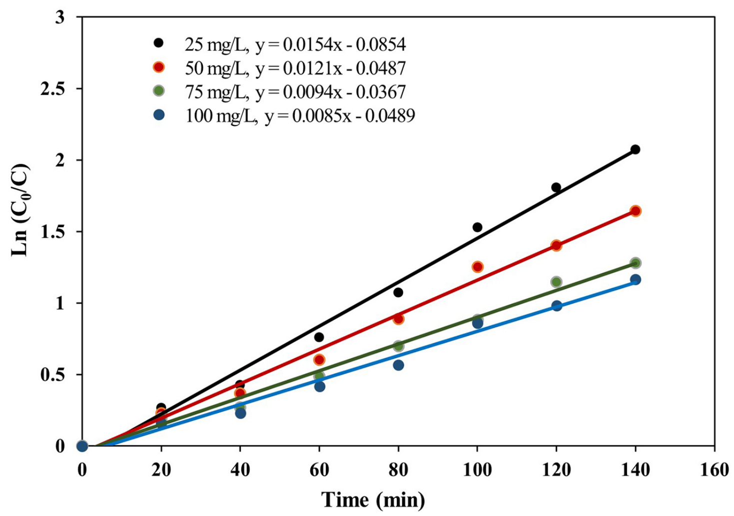

Figure 9. Kinetic photocatalytic degradation of MO by $CoFe_2O_4$-SiO_2-TiO_2

Table 3. Kinetic parameter of photocatalytic degradation MO

MO (mg/L)	R^2	k (min^{-1})	$t_{1/2}$ (min)
25	0.9902	0.0154	45.0
50	0.9909	0.0121	57.3
75	0.9907	0.0094	73.7
100	0.9859	0.0085	81.5

discharge of secondary pollutants into the environment. Photocatalytic degradation is carried out using a MO concentration of 25 mg/L, a pH of 4, a catalyst dose of 0.05 g/L, as well as an irradiation time of 160 minutes. According to Figure 10, the catalyst effectiveness reduced by 3.74%, from 93.46% to 89.96%, after 5 cycles. Moosavi et al. [2020] reported similar results in the effectiveness of Fe_3O_4/AC/TiO_2 in photocatalytic degradation which reduced from approximately 98% to about 93% after 7 cycles. This study obtained better results, compared to MO degradation using Ti_2-Fe_3O_4-bentonite, where the catalyst effectiveness decreased by approximately 20% after 6 cycles. Furthermore, the reduction in the catalyst effectiveness is possibly due to the loss of material during the photocatalytic degradation process (separation, washing, and drying), as well as the occurrence of catalyst aggregation.

A total organic carbon (TOC) analysis was also performed to determine the amount of organic matter or the level of mineralization. According to Pourzad et al., [2020], the level of mineralization is usually not fully achieved. The TOC efficiency on photocatalytic degradation of methylene blue dye using Ag_2O-NiO/$CuFe_2O_4$ catalyst is 78.64% [Liu et al., 2020], while the TOC efficiency of paraquat using N-doped TiO_2-SiO_2-Fe_3O_4 is 84.71% [Pourzad et al., 2020]. In this study, the efficiency of TOC removal for photocatalytic degradation of MO under optimal conditions with a concentration of 25 mg/L, catalyst dose of 0.05 g/L, solution pH of 4, and irradiation time of 160 minutes is 82.68%. This result indicates a successful dye decomposition process.

CONCLUSIONS

A core-shell-shell composite in the form of $CoFe_2O_4$-SiO_2-TiO_2 was successfully synthesized and effectively used for photocatalytic degradation of methyl orange dye under UV light irradiation. On the basis of the XRD analysis, $CoFe_2O_4$ was discovered to possess a cubic spinel structure and TiO_2 was in the anatase phase. In addition, the FTIR and SEM-EDS analyses confirmed the presence of SiO_2 and TiO_2 shells. The $CoFe_2O_4$-SiO_2-TiO_2 composite possessed magnetic properties with a saturation magnetization of 47 emu/g, as well as a bandgap of 2.4 eV. Furthermore, the removal efficiency of MO using $CoFe_2O_4$-SiO_2-TiO_2 was discovered to be 93.46% with a MO concentration of 25 mg/L, solution pH of 4, catalyst dose of 0.05 g/L, and irradiation time of 160 minutes under UV light irradiation. In addition, the photocatalytic degradation followed the Langmuir-Hinshelwood model expressed in pseudo-first-order. These results show that $CoFe_2O_4$-SiO_2-TiO_2 has the potential for use in wastewater treatment, especially for organic pollutant removal. The catalyst effectiveness decreased by only 3.74% after 5 cycles of photocatalytic degradation.

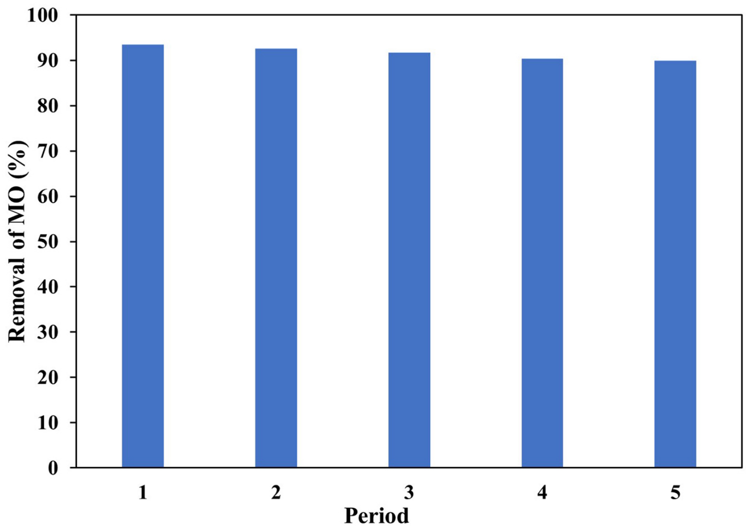

Figure 10. Reusability of the $CoFe_2O_4$-SiO_2-TiO_2 photocatalyst

Acknowledgement

The authors are grateful to the *Kemendikbud Ristek* for the provision of financial aid towards this study, under the *Penelitian Dasar Unggulan Perguruan Tinggi* scheme with Contract No. 0166.15/UN9/SB3.LP2M.Pt/2021.

REFERENCES

1. Ahmad M., Ahmed E., Hong Z.L., Ahmed W., Elhissi A., Khalid N.R. 2014. Photocatalytic, sonocatalytic and sonophotocatalytic degradation of Rhodamine B using ZnO/CNTs. Ultrasonics Sonochemsitry, 21(2), 761–773.
2. Ajabshir S.Z., Niasari M.S. 2019. Preparation of magnetically retrievable $CoFe_2O_4$-SiO_2-$Dy_2Ce_2O_7$ nanocomposites as novel photocatalyst for higly efficient degrdation of organic contaminants. Composites Part B: Engineering, 174, 1–9.
3. Ajmal A., Majeed I., Malik R.N., Idriss H., Nadeem M.A. 2014. Principles and mechanisms of photocatalytic dye degradation on TiO_2 based photocatalytic a comparative overview. RSC Advances, 4, 37003–37026.
4. Alghamdi A.A., Al-Odayni A.B., Saeed W.S., Almutairi MS., Alharthi, F.A.A, Aouak T., Al-Kahtani AA. 2019. Adsorption of azo dye Methyl Orange from aquaeous solutions using alkali-activated polypyrrole-based graphene oxide. Molecules, 24, 1–17.
5. Amulya M.A.S., Nagaswarupa H.P., Kumar M.R.A., Ravikumar C.R., Prashantha S.C., Kusuma KB. 2020. Sonochemical synthesis of $NiFe_2O_4$ nanoparticles: Characterization and their photocatalytic and electrochemical applications. Applied Surface Sciences Advances, 1, 1–10.
6. Awazu K., Fujimahi M., Rockstuhi C., Tominaga J., Murakami H., Ohki Y. 2008. A plasmonic photocatalyst consisting of silver nanoparticles embedded in titanium dioxide. Journal of the American Chemical Society, 130(5), 1676–1680.
7. Behzadi S., Nonahal B., Royaee S.J., Asadi A.A. 2020. TiO_2-SiO_2-Fe_3O_4 magnetic nanoparticles synthesis and appication in methyl orange photocatalytic removal. Water Science & Technology, 82 (11), 2432–2445.
8. Chan T., Zheng Y., Lin J.M., Chen G. 2008. Study on the photocatalytic degradation of Methyl Orange in water using Ag-ZnO as catalyst by Liquid Chromatograpgy Electrospray Ionization Ion-Trap Mass Spectrometry. Journal of the American Society for Mass Spectrometry, 19, 997–1003.
9. Chen W., Xiao H., Xu H., Ding T., Gu Y. 2015. Photodegrdation of Methylene Blue by TiO_2-Fe_3O_4-Bentonite magnetic nanocomposite. International Journal of Photoenergy, 2015, 1–7.
10. Cheng J., Ma R., Li M., Wu J., Liu F., Zhang X. 2012. Anatase nanocrystals coating on silica-coated magnetite: role of polyacrylic acid treatment and its photocatalytic properties. Chemical Engineering Journal, 210(7), 80–86.
11. Djellabi, R., Yang, B., Wang, Y., Cui, X., Zhao, X. 2019. Carbonaceous biomass-titania composites with Ti–O–C bonding bridge for efficient photocatalytic reduction of Cr(VI) under narrow visible light. Chemical Engineering Journal, 366, 172–180.
12. El-Shobaky G., Turky A., Mostafa N., Mohamed S. 2010. Effect of preparation conditions on physicochemical, surface and catalytic properties of cobalt ferrite prepared by coprecipitation. Journal of Alloys and Compounds, 493, 415–422.
13. Fu C., Liu X., Wang Y., Li L., Zhang Z. 2019. Preparation and characterization of Fe_3O_4-SiO_2-TiO_2-CorGO magnetic visible light photocatalyst for water treatment. RSC Advances, 9, 20256–20265.
14. Gebrezgiabher M., Gebreslassie G., Gebretsadik T., Yeabyo G., Elemo F., Bayeh Y., Thomas M., Linert W. 2019. AC-Doped TiO_2-Fe_3O_4 Nanocomposite for Photocatalytic Dye 2018. Degradation under Natural Sunlight Irradiation. Journal of Composite Science, 3(3), 1–11.
15. Ge J., Zhang Y., Heo Y.J., Park S.J. 2019. Advanced design and synthesis of composite photocatalysts for the remediation of wastewater: a review. Catalysts, 9(2), 1–32.
16. Habila M.A., Al-Othman Z.A., El-Toni A.M., Labis J.P., Soylak M. Synthesis and application of Fe_3O_4-SiO_2-TiO_2 for photocatalitic decomposition of organic matrix simultaneously with magnetic solid phase extraction of heavy metals prior to ICP-MS analysis. Talanta, 154, 539–547.
17. Huang J.H., Huang K.L., Liu S.Q., Wang A.T., Yan C. 2008. Adsorption of Rhodamine B nad Methyl Orange on a hypercrosslinked polymer adsorbent in aqueous solution. Colloids and Surfaces A: Physicochemical and Engineering Aspects, 330(1), 55–61.
18. Houshiar M., Zebhi F., Razi Z.J., Alidoust A., Askari Z. 2014. Synthesis of cobalt ferrite ($CoFe_2O_4$) nanoparticles using combustion, coprecipitation, and precipitation methods: A comparison study of size, structural, and magnetic properties. Journal of Magnetism and Magnetic Materials, 371, 43–48.
19. Jurek A.Z., Bielan Z., Dudziak S., Wolak I., Sobczak T., Klimczuk T., Nowaczyk G., Hupka J. 2017. Design and application of magnetic photocatalysts for water treatment. The effect of particle charge on surface functionality. Catalysts, 360(7), 1–18.
20. Jorfi S., Kakavandi B., Motlagh H.R., Jaafarzadeh N. 2017. A novel combination of oxidative degradation for benzotriazole removal using TiO_2 loaded on $Fe^{II}Fe_2^{III}O_4$-C as an efficient activator of peroxymonosulfate. Applied Catalysis B: Environmental, 219, 216–230.

21. Konstantinou I.K., Albanis T.A. 2004. TiO_2-assisted photocatalytic degradation of azo dyes in aqueous solution: Kinetic and mechanistic investigations. Applied Catalysis B: Environmental, 49, 1–14.
22. Koohestani H., Sadrnezhaad S.K. 2016. Photocatalytic degradation of Methyl Orange and Cyanide by Using TiO_2-CuO composite. Desalination and Water Treatment, 2016, 1–10.
23. Lee S.A., Choo K.H., Lee CH., Lee H.I., Hyeon T., Choi W., Kwon H.H. 2001. Use of ultrafiltration membranes for the separation of TiO_2 photocatalysts in drinking water treatment. Industrial & Engineering Chemistry Research, 40(7), 1712–1719.
24. Liu L., Hu N., An Y., Du X., Zhang X., Li Y., Zeng Y., Cui Z. 2020. Ag_2O and NiO decorated $CuFe_2O_4$ with enhaced photocatalytic performance to improve the degradation efficiency of Methylene Blue. Materials, 13, 1–12.
25. Mercyrani B., Maya R.H., Lopez M.S., Th-Th C., Velumani S. 2017. Photocatalytic degrAdation of Orange G using TiO_2-Fe_3O_4 nanocomposite. Journal of Materials Science: Materials in Electronics, 29, 15436–15444.
26. Mishra P., Patnaik S., Parida K. 2019. An overview of recent progresses on noble metal modified magnetic Fe_3O_4 for photocatalytic pollutant degradation and H_2 evolution. Catalysis Science & Technology, 9, 916–941.
27. Moosavi S., Li R.Y.M., Lai C.W., Yusof Y., Gan S., Akbarzadeh O., Chowhury Z.Z., Yue X.G, Johan M.R. 2020. Methylene blue dye photocatalytic degradation over synthesises Fe_3O_4-AC-TiO_2 nanocatalyst: Degrdation and reusability Studies. Nanomaterials, 10(12), 1–15.
28. Mortazavi D.S., Salavati D.M., Abbasi N.O.A.A. 2017. Fabrication and characterization of Fe_3O_4-SiO_2-TiO_2-Ho nanostructures as a novel and highly efficient photocatalyst for degradation of organic pollution. Journal of Energy Chemistry, 26(1), 17–23.
29. Mrotek E., Dudziak S., Malinowska I., Pelczarski D., Ryzynska Z., Juruk A.Z. 2020. Improved degradation of etodolac in the presence of core-shell $ZnFe_2O_4$-SiO_2-TiO_2 magnetic photocalyst. Science of The Total Environment, 724, 1–12.
30. Nair P.G., Vijayakumar S., Lisluke T., Mathew M.S.P, Aravindakumar CT. 2014. Degradation of dyestuff pollutant Sudan I using advanced oxidation process. Journal of water Resource and Protection, 6(14), 1276–1283.
31. Ojemaye, M.O., Okoh O.O., Okoh A.I. 2017. Performance of $NiFe_2O_4$-SiO_2-TiO_2 magnetic photocatalyst for the effective photocatalytic reduction of Cr(VI) in aquation solutions. Journal of Nanomaterials, 2017, 1–11.
32. Pastravanu C.C., Ignat M., Popovici E., Harabagiu V. 2014. TiO_2-coated mesoporous carbon: Conventional vs. microwave-annealing process. Journal of Hazardous Materials, 278, 382–390.
33. Pourzad A., Sobhi H.R., Behbahani M., Esrafili A., Kalantary R.R., Kermani M. 2020. Efficient visible light-induced photocatalytic removal of paraquat using N-doped TiO_2-SiO_2-Fe_3O_4 nanocomposite. Journal of Molecular Liquids, 299, 1–7.
34. Rashid J., Barakat M.A., Ruzmanova Y., Chianese A. 2015. Fe_3O4-SiO_2-TiO_2 nanoparticles for photocatalytic degradation of 2-chlorophenol in simulated wastewater. Environmental Science and Pollution Research, 22, 3149–3157.
35. Rajput J.K., Kaur G. 2014. Synthesis and applications of $CoFe_2O_4$ nanoparticles for multicomponent reaction. Catalysis Science & Technology, 4, 142–151.
36. Shojaie A., Fattahi M., Jorfi S., Ghasemi B. 2018. Synthesis and evaluations of Fe_3O_4-TiO_2-Ag nanocomposites for photocatalytic degradation of 4-chlorophenol (4-CP): effect of Ag and Fe compositions. International Journal of Industrial Chemistry, 9, 141–151.
37. Stefan M., Leostean C., Pana O., Toloman D., Popa A., Perhaita I., Senila M., Marincas O., Tudoran LB. 2016. Magnetic recoverable Fe_3O_4-TiO_2: Eu composite nanoparticles with enhanced photocatalytic activity. Applied Surface Science, 390, 248–259.
38. Subramonian W., Wu T.Y., Chai S.P. 2017. Photocatalytic degradation of industrial pulp and paper mill effluent using synthesized magnetic Fe_2O_3-TiO_2: Treatment efficiency and characterizations of reused photocatalyst. Journal of Environmental management, 187, 298–310.
39. Suzuki H., Araki S., Yamamoto H., 2015. Evaluation of advanced oxidation processes (AOP) using O_3, UV, and TiO_2 for the degradation of phenol in water. Journal of Water Process Engineering, 7, 54–60.
40. Sonu, Duta V., Sharma S., Raizada P., Bandeghараеi A.H., Gupta V.K., Singh P. 2019. Review on augmentation in photocatalytic activity of $CoFe_2O_4$ via heterojunction formation for photocatalysis of organic pollutants in water. Journal of Saudi Chemical Society, 23, 1119–1136.
41. Takdastan A., Kakavandi B., Azizi M., Golshan M. 2018. Efficient activation of peroxymonosulfate by using ferroferric oxide supported on carbon/UV/US system: A new approach into catalytic degradation of bisphenol A. Chemical Engineering Journal, 331, 729–743.
42. Trabelsi H., Atheba G.P., Hentati O, Meriette Y.D, Robert D, Drogui P., Ksibi M. 2016. Solar photocatalytic decolorization and degradation of Methyl Orange using supported TiO_2. Journal of Advanced Oxidation Technologies, 19 (1), 79–84.
43. Wysocka I., Kowalska E., Trzcinski K., Lapinski M., Nowaczyk G., Jurek A.Z. 2018. UV-vis-induced degradation of phenol over magnetic photocatalysts modified with Pt, Pd, Cu and Au nanoparticles. Nanomaterials, 8(1), 1–20.